American Journal of Human Genetics, Volume *82*

Supplemental Data

Loss of Nephrocystin-3 Function Can Cause Embryonic Lethality, Meckel-Gruber-like Syndrome, Situs Inversus, and Renal-Hepatic-Pancreatic Dysplasia

Carsten Bergmann, Manfred Fliegauf, Nadina Ortiz Brüchle, Valeska Frank, Heike Olbrich, Jan Kirschner, Bernhard Schermer, Ingolf Schmedding, Andreas Kispert, Bettina Kränzlin, Gudrun Nürnberg, Christian Becker, Tiemo Grimm, Gundula Girschick, Sally A Lynch, Peter Kelehan, Jan Senderek, Thomas J Neuhaus, Thomas Stallmach, Hanswalter Zentgraf, Peter Nürnberg, Norbert Gretz, Cecilia Lo, Soeren Lienkamp, Tobias Schäfer, Gerd Walz, Thomas Benzing, Klaus Zerres, and Heymut Omran

A

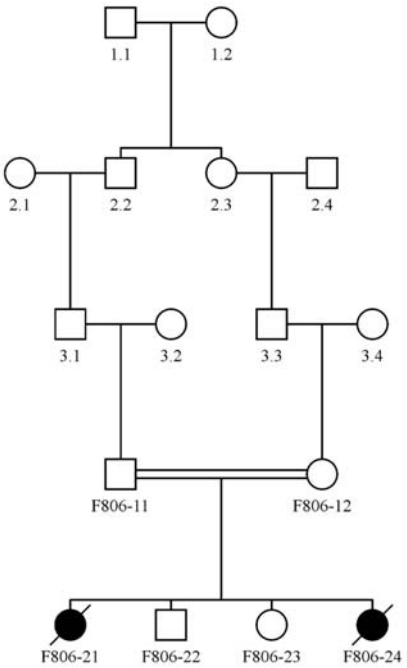
1.1
1.2
2.1
2.2
2.3
2.4
3.1
3.2
3.3
3.4
F806-11
F806-12
F806-21
F806-22
F806-23
F806-24

B

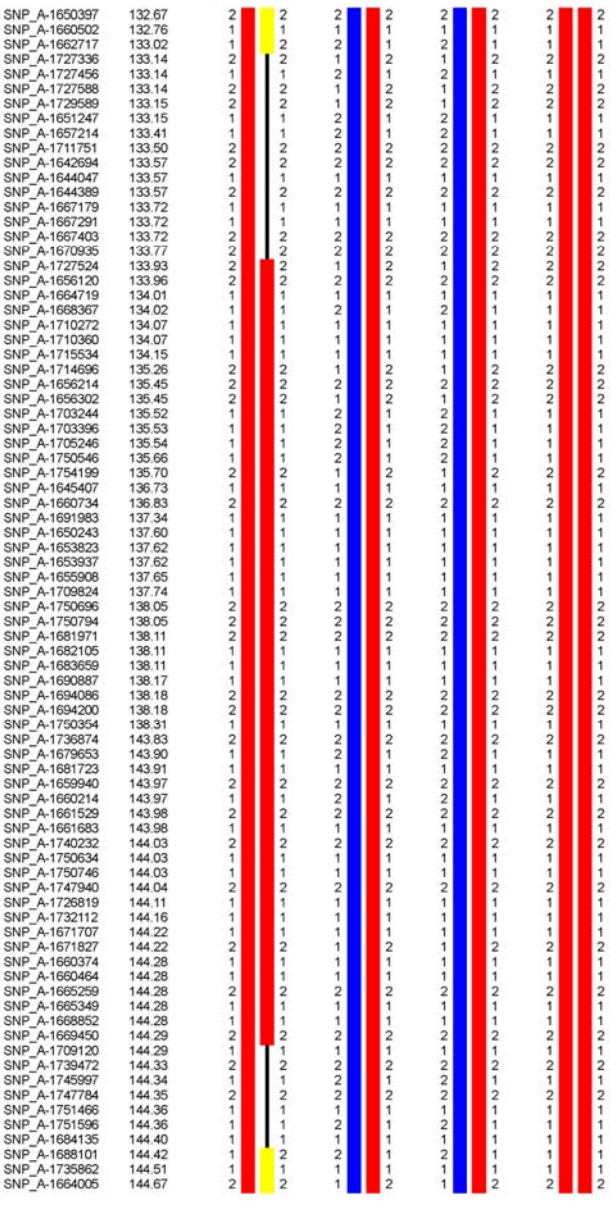
SNP_A-1650397 132.67
SNP_A-1660502 132.76
SNP_A-1662717 133.02
SNP_A-1727336 133.14
SNP_A-1727456 133.14
SNP_A-1727588 133.14
SNP_A-1729589 133.15
SNP_A-1651247 133.15
SNP_A-1657214 133.41
SNP_A-1711751 133.50
SNP_A-1642694 133.57
SNP_A-1644047 133.57
SNP_A-1644389 133.57
SNP_A-1667179 133.72
SNP_A-1667291 133.72
SNP_A-1667403 133.72
SNP_A-1670935 133.77
SNP_A-1727524 133.93
SNP_A-1656120 133.96
SNP_A-1664719 134.01
SNP_A-1668367 134.02
SNP_A-1710272 134.07
SNP_A-1710360 134.07
SNP_A-1715534 134.15
SNP_A-1714696 135.26
SNP_A-1656214 135.45
SNP_A-1656302 135.45
SNP_A-1703244 135.52
SNP_A-1703396 135.53
SNP_A-1705246 135.54
SNP_A-1750546 135.66
SNP_A-1754199 135.70
SNP_A-1645407 136.73
SNP_A-1660734 136.83
SNP_A-1691983 137.34
SNP_A-1650243 137.60
SNP_A-1653823 137.62
SNP_A-1653937 137.62
SNP_A-1655908 137.65
SNP_A-1709824 137.74
SNP_A-1750696 138.05
SNP_A-1750794 138.05
SNP_A-1681971 138.11
SNP_A-1682105 138.11
SNP_A-1683659 138.11
SNP_A-1690887 138.17
SNP_A-1694086 138.18
SNP_A-1694200 138.18
SNP_A-1750354 138.31
SNP_A-1736874 143.83
SNP_A-1679653 143.90
SNP_A-1681723 143.91
SNP_A-1659940 143.97
SNP_A-1660214 143.97
SNP_A-1661529 143.98
SNP_A-1661683 143.98
SNP_A-1740232 144.03
SNP_A-1750634 144.03
SNP_A-1750746 144.03
SNP_A-1747940 144.04
SNP_A-1726819 144.11
SNP_A-1732112 144.16
SNP_A-1671707 144.22
SNP_A-1671827 144.22
SNP_A-1660374 144.28
SNP_A-1660464 144.28
SNP_A-1665259 144.28
SNP_A-1665349 144.28
SNP_A-1668852 144.28
SNP_A-1669450 144.29
SNP_A-1709120 144.29
SNP_A-1739472 144.33
SNP_A-1745997 144.34
SNP_A-1747784 144.35
SNP_A-1751466 144.36
SNP_A-1751596 144.36
SNP_A-1684135 144.40
SNP_A-1688101 144.42
SNP_A-1735862 144.51
SNP_A-1664005 144.67

Figure S1. Pedigree and Linkage Analysis in Family F806

(A) Pedigree of consanguineous multiplex family F806.

(B) GENEHUNTER haplotypes of the four children of family F806 for the locus on chromosome 3q21.2-q22.3 obtained by genome-wide SNP mapping with the 50K Affymetrix SNP array. This locus was subsequently confirmed by microsatellite marker analysis and refined to an 11.6 Mb interval flanked by rs905455 and D3S1216.

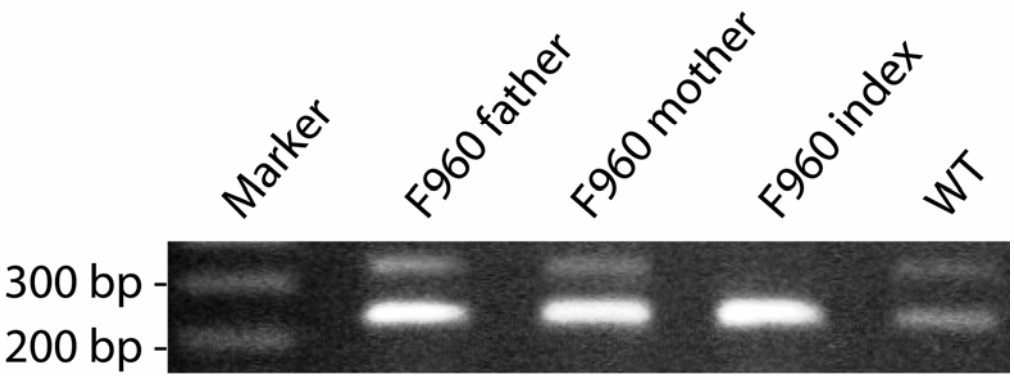

Figure S2. Homozygous Splice Mutation in Family F960

Characterization of the donor splice mutation c.1985+5G → A in family 960 on RNA level with primers in exons 11 and 14. RT-PCR products from parental lymphocytes were compared with control lymphocytes. Sequencing demonstrated that the upper band that is present in the patient's parents and control but not in the patient corresponded to the wild-type (WT) complementary DNA (cDNA) sequence comprising exons 11–14. The lower band corresponded to skipping of exon 13 and is predicted to result in an out-of-frame transcript and premature termination of translation, confirming the pathogenicity of this homozygous mutation in the proposita.

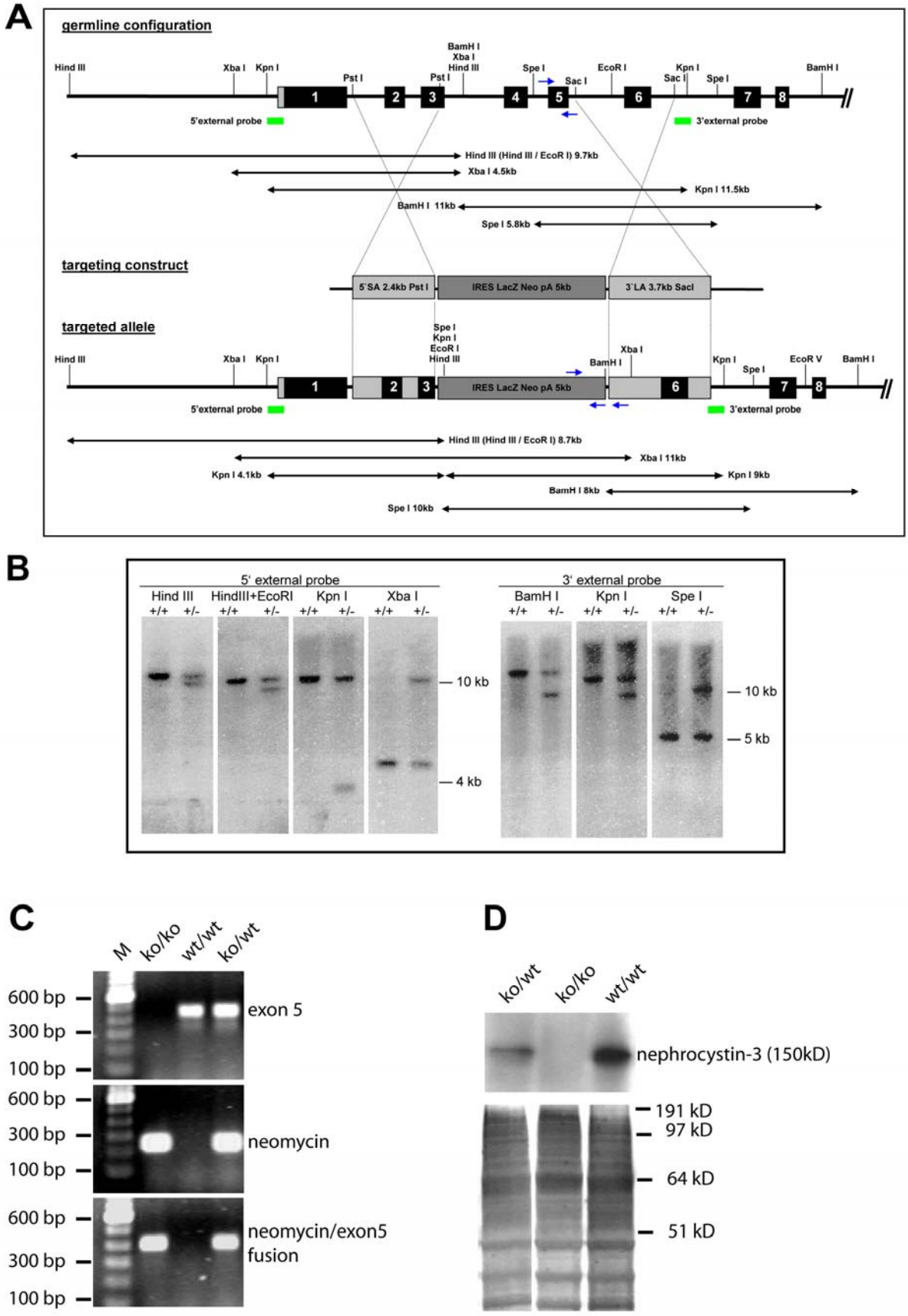

Figure S3. Generation of *Nphp3* ko Mice by Gene Targeting

(A) Schematic diagram of the *Nphp3* locus (Exons 1–8 are shown only), the targeting vector, and the targeted allele. Only the relevant restriction enzyme sites are indicated. The expected band sizes that correspond to the wild-type and mutated genotypes, respectively, are indicated by vertical arrows.

(B) G418-resistant embryonic stem (ES) cell clones with a correctly targeted *Nphp3* locus were identified by Southern-blot analysis of restriction-enzyme-digested ES cell genomic DNA as indicated. The correct structure of the targeted locus on both sides was confirmed with a 5′ external and a 3′ external probe, which hybridized to fragments of the predicted sizes for the wild-type allele and a correctly targeted allele. The existence of a single integration site at the targeted locus was verified with an internal probe derived from the resistance cassette (data not shown). A homologously targeted ES cell clone was injected into C57BL/6 blastocysts, and chimeric mice were bred to C57BL/6 mice, yielding mice heterozygous for the mutant allele. Heterozygous mice were backcrossed to C57BL/6 mice for six generations and interbred so that embryos homozygous for the mutant allele could be obtained. All animals were kept under specific pathogen-free conditions.

(C) Mice and embryos were genotyped from tail DNA and yolk-sack DNA, respectively, by PCR with primers specific for exon 5, the neomycin gene, and the neomycin/intron 5 fusion region (primer locations are indicated in (A) by short blue arrows). Size markers are shown on the left side.

(D) The generation of a null allele was confirmed by western blot with mouse monoclonal antibodies raised against a 253 amino acid C-terminal fragment derived from the highly homologous human nephrocystin-3. Genotyped embryos (E12.5) were homogenized in RIPA-buffer, and proteins were separated and blotted with a NuPAGE gel system (Invitrogen, Karlsruhe, Germany). The polyvinylidene fluoride (PVDF) membrane was processed for enhanced chemiluminescence (ECL) detection (both GE Healthcare, Freiburg, Germany) with horseradish peroxidase (HRP)-conjugated secondary antibodies (SantaCruz Biotechnology, Heidelberg, Germany). Nephrocystin-3 is decreased in the heterozygous embryo, absent in the homozygous embryo, and readily detectable in the wild-type embryo (top). Equal loading and protein integrity was confirmed by silverstaining of aliquots run on a separate gel (bottom). Molecular weight markers are indicated on the right.

Table S1. Primer Pairs Used for *NPHP3* Mutation Analysis

		Primer Sequences	
Exon	**Size (bp)**	**Forward (5′-3′)**	**Reward (5′-3′)**
1	496	CACTAGGTAGTAGCGGCAACG	AAGCCGCTTGGTTTGGAG
2	400	GGCAACATGAAGTTCCTGATAA	ACTTTCCTGAATCCTACATGACTT
3	400	GAAATCGAGGACCAAATGAA	CTATTTGCAACAGTAGTTAAAGCAA
4	400	GTCGATGGCAAAGTATTTTCA	TTTCATGCTTTGCTAATGGTATT
5	370	GATTCCATTCTATGATGCCTGTT	CCAAGACGCTTCCTGTTCTT
6	392	TGTTTTAAAGCGTGCTTTTTATT	GTTGTAGAATTTATTGAATTTCATGG
7	393	ACCTTTTCTGGCCACTTGTC	CCAGCCACACTGGTTTCTCT
8	393	ATCCCTTGTGTGACCTTGGA	CAAGCAAGTGGTTTTCTCTGG
9	398	GTAGGTGAAGCCCACTTTGG	CATGGATAATCAAGCCATGAGA
10	299	TCATTTTCTCACACAGCTTTTCTC	GGCAGGCATGCAATACATTT
11/12	698	GGCAACATTTGATGTTTACTGC	GCCTGCTCTAGCTATTACTGAATTT
13	357	CACCCCAAAATAAGATTTTTATCC	CACTTCTCCCCATCCTCACT
14/15	814	AAGCAGTATAAAGTGTTAATTCCTGTG	GTTTTGCAGGGTGAGAAAGG
16	375	TTGAATTTGTTATTGGTTGCAGT	TCCTGCATATGCCTGAAACA
17	364	TTGGTAAAAAGAAATAGCCTTAAAAGA	GGCAGAAATAATCTTGCCACT
18/19	978	TTTTTGCAAATCTCTTGTTAGATG	AAATTGTCTCAAGATTTCTCCTACACT
20/21	847	TGAGTGGTCTGAGTCTTACCTCA	CACAGTGATAAAACAAAGCTTACCC
22/23	1190	GCCCAAAAAGACTTTACACTATGAA	CATGAAATTTTGCGTGGTTTT
24	500	GAGATAGGGGTGGGGAAGAG	ACCTGTCCCTCATAAAGACAAA
25/26	1000	TTTTCCCTCAAAATTACCCTTT	TGTGCTATTCTAAGACAAAGCTACTTC
27	460	AGAGGGGAAATGGGCAAATA	CACAATTCCAACTTAATGTAATCCA

GenBank NM_153240. Annealing temperature for all PCR fragments was 58°C.